



Design and fabrication of integrated micro/macrostructure for 3D functional gradient systems based on additive manufacturing



Ming Yin ^{*}, Luofeng Xie, Weifeng Jiang, Guofu Yin

School of Manufacturing Science and Engineering, Sichuan University, Chengdu, 610065, China

ARTICLE INFO

Keywords:

3D functional gradient system
Metamaterials
Additive manufacturing
Photonic crystals

ABSTRACT

Functional gradient systems have important applications in many areas. Although a 2D dielectric structure that serves as the gradient index medium for controlling electromagnetic waves is well established, it may not be suitable for application in 3D case. In this paper, we present a method to realize functional gradient systems with 3D integrated micro/macrostructure. The homogenization of the structure is studied in detail by conducting band diagram analysis. The analysis shows that the effective medium approximation is valid even when periodicity is comparable to wavelength. The condition to ensure the polarization-invariant, isotropic, and frequency-independent property is investigated. The scheme for the design and fabrication of 3D systems requiring spatial material property distribution is presented. By using the vat photopolymerization process, a large overall size of macrostructure at the system level and precise fine features of microstructure at the unit cell level are realized, thus demonstrating considerable scalability of the system for wave manipulation.

© 2018 Elsevier B.V. All rights reserved.

1. Introduction

Systems with designed and engineered distribution of gradient material property offer unprecedented opportunities to achieve required functions, which have important implications for a multitude of disciplines in today's scientific and engineering world. In many functional devices, the integration of dissimilar materials could result in an incompatible interface. Engineered material property transitions across the interface can reduce the mismatches in electromagnetic, mechanical, or thermal properties. Graded transitions can also enhance the mechanical performance of the interface to prevent premature failure by reducing stress concentrations, redistributing thermal stresses, or improving interfacial bonding [1,2]. Controlled material property gradients over volume has also been used in structural engineering applications, for example, to produce artificial body for soft robot or biomaterial for medical applications [2–4]. Moreover, devices with specific gradient distribution of material properties enable the control of electromagnetic, thermodynamic, or mechanical wave propagation in desired ways [5–9].

Such functional gradient systems would usually require complex material parameters and precise control of property distribution. The distribution of material properties can be engineered by continuously varying the composition or microstructure of the constituent materials

over volume. Such functionally graded materials can be realized by the composite material synthesis approach, which normally involves complex manufacturing techniques. The development of new fabrication techniques such as the multimaterial additive manufacturing process offers the ability to fabricate functionally graded parts with controllable shape and material performance [3,4]. However, the state of the art is still limited for the real application aspect. More available materials and comprehensive processing capabilities would be required to develop functional parts with precise control of complex structure and gradient property from laboratory samples with relatively simple morphology and discrete material property distribution.

Metamaterial provides a promising approach to construct functional gradient systems. By using the principle of metamaterial, the required gradient property distribution can be realized by spatially changing the subwavelength structure rather than the composition or microstructure of constituent materials, which would then ease the challenge for fabrication. The principle of metamaterial can be applied to different areas [7–9], but in the present study, we mainly focus on the 3D electromagnetic gradient systems. In electromagnetism, the planar gradient metamaterials with 2D or 2.5D geometry are well established [10–14]. However, when they are applied to complex 3D systems, the out-of-plane propagation cannot be ignored, and the incident angle or polarization of wave may be limited. Moreover, metamaterials constructed

^{*} Corresponding author.

E-mail address: mingyin@scu.edu.cn (M. Yin).

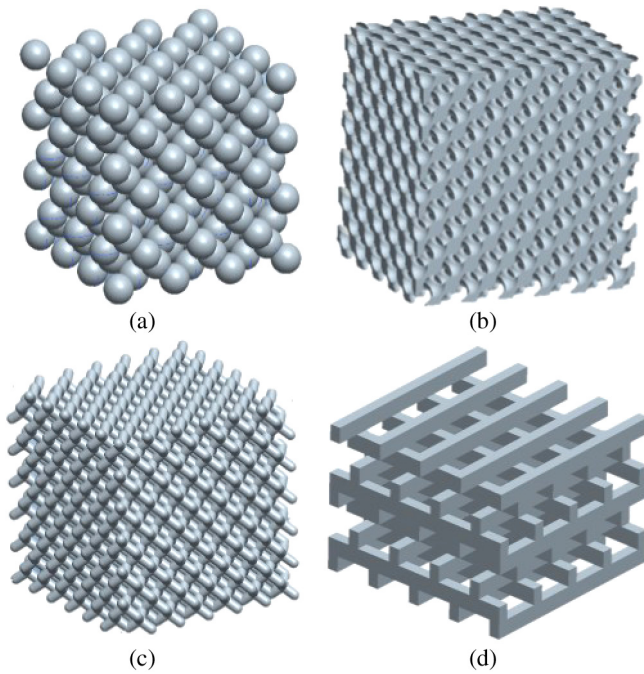


Fig. 1. Typical 3D dielectric structures. (a) Dielectric spheres arranged in the lattice. (b) Air spheres arranged in the lattice. (c) Rod-connected structure. (d) Woodpile structure.

using dielectrics without metallic inclusions can enable to realize broadband and low-loss property at optical frequencies. Therefore, dielectric structures with 3D topology are expected to be good candidates for 3D systems.

In this paper, we present a method to realize 3D functional gradient system with 3D integrated micro- and macrostructure. The homogenization of the structure is studied using band diagram calculations. The condition to validate the effective medium approximation and to ensure the polarization-invariant, isotropic, and frequency-independent property is investigated and discussed in detail. The required spatial material property distribution is realized with integrated micro/macrostructure. The scheme for the design and fabrication of such systems is presented. The vat photopolymerization-based additive manufacturing process is used in the implementation. Large overall size at the system level and fine features at the unit cell level are realized, thus demonstrating considerable scalability of the system for wave control.

2. Homogenization of the 3D periodic dielectric structure

Artificial dielectric structure can be homogenized and can serve as a gradient index medium in the long-wavelength regime. A 2D case in this regime has been studied in detail [14–18], and a 3D case has also been previously realized [19]. For a 3D periodic dielectric structure to serve as an effective medium, properties such as polarization independence, isotropy, and non-dispersion are expected in unit cells with high-symmetry geometry. To satisfy the effective medium approximation, it is usually required that the periodicity should be one order of magnitude smaller than the free-space wavelength. Moreover, when the ratio of periodicity to wavelength is not negligible, it will reach the photonic crystal regime, where the Bragg diffraction mechanism becomes significant. However, the effective medium limit for the 3D dielectric structure is not that strict [19]. We conduct band diagram-based calculations to study this point in detail. Typical 3D dielectric structures with high-symmetry face-centered cubic (FCC) lattice [20,21] are presented in Fig. 1.

As discussed in Section 3, such periodic structures with gradient topology can be realized by photopolymerization-based 3D fabrication

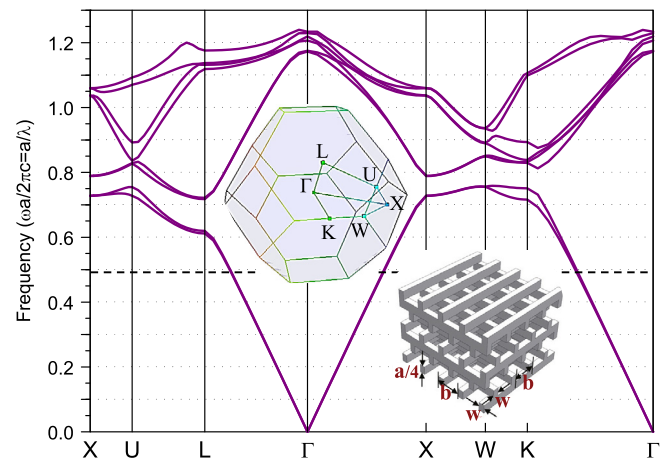


Fig. 2. Band diagrams for the lowest first and second bands. Upper left inset: symmetry k -points in the Brillouin zone of the FCC lattice. Lower right inset: illustration of structural parameters for the woodpile structure.

techniques such as the direct laser writing or the vat photopolymerization process. In the structure design, the available fabrication capabilities should be considered. Dielectric structures with self-supporting topologies, without the need of a substrate, would ease the fabrication and be suitable as a 3D gradient medium. Fig. 1(a) shows the structure of dielectric spheres arranged in the lattice. The radius of each sphere embedded in air should be large enough to cause overlap and create connected networks. A structure that allows a larger range of dielectric volume fraction is preferred to achieve more flexible control of effective material property. However, in this case, low dielectric volume fraction cannot be realized. Fig. 1(b) shows the structure of air spheres arranged in the lattice. For the photopolymerization-based processes, the unexposed material that exists in the enclosed structure cannot be removed during or after fabrication. Therefore, in this case, the radius of each air sphere should be large enough to avoid undesirable enclosed cavities in the integrated structure, and high dielectric volume fraction cannot be realized. Fig. 1(c) and (d) present the so-called rod-connected and woodpile structures, respectively. For these two cases, the dielectric volume fraction can be theoretically tuned from 0 to 1 because the dielectric rods would always remain connected and make the structure self-supporting.

Compared with the rod-connected structure, the woodpile structure is simpler in geometry and easier to fabricate. It is studied as a proof-of-principle. When the rod thickness is $a/4$ and the rod spacing b is $a/\sqrt{2}$, the lattice is strictly FCC with the lattice constant of a . If the rod width is set to be w , then the dielectric volume fraction can be controlled by varying the w/b ratio. Lossless and non-dispersive material with permittivity of 3 (a typical value for photopolymer [22]) is applied as the constituent material. The band diagram-based calculations are conducted using BandsOLVE. The calculated band diagrams for the lowest bands are shown in Fig. 2. In general, when the normalized frequency is relatively low, the lowest first and second bands are very closely spaced and compromise a degenerate pair, indicating that the unit cell with high symmetry is polarization invariant at long wavelength. Moreover, the dispersion relationship $\omega(\mathbf{k})$ is linear, indicating that the structure can be homogenized as a non-dispersive effective medium in a broadband as expected.

The dispersion curves for the wave vector \mathbf{k} moving from the origin Γ to the special symmetry points at the irreducible Brillouin zone (K, W, X, U , and L , respectively) are plotted in Fig. 3. As shown in Fig. 3(a) and (b), for $\mathbf{k}_{\Gamma-X}$ and $\mathbf{k}_{\Gamma-L}$, where \mathbf{k} moves from Γ towards the face center of the Brillouin zone, the first and second bands nearly remain degenerate for the whole Brillouin zone. As shown in Fig. 3(c)–(e), for $\mathbf{k}_{\Gamma-U}$, $\mathbf{k}_{\Gamma-K}$, and $\mathbf{k}_{\Gamma-W}$ (where U, K , and W are the symmetry points

Download English Version:

<https://daneshyari.com/en/article/7925674>

Download Persian Version:

<https://daneshyari.com/article/7925674>

[Daneshyari.com](https://daneshyari.com)